Cell Stem Cell
Article

The Death Receptor CD95 Activates Adult Neural Stem Cells for Working Memory Formation and Brain Repair

Nina S. Corsini,[1] Ignacio Sancho-Martinez,[1] Sabrina Laudenklos,[1] Désirée Glagow,[1] Sachin Kumar,[1] Elisabeth Letellier,[1] Philipp Koch,[6] Marcin Teodorczyk,[1] Susanne Kleber,[1] Stefan Klussmann,[1] Benedict Wiestler,[1] Oliver Brüstle,[6] Wolf Mueller,[8] Christian Gieffers,[5] Oliver Hill,[5] Meinolf Thiemann,[5] Matthias Seedorf,[2] Norbert Gretz,[7] Rolf Sprengel,[3] Tansu Celikel,[4] and Ana Martin-Villalba[1,*]

[1]Molecular Neurobiology, German Cancer Research Center, 69120 Heidelberg, Germany
[2]Zentrum für Molekulare Biologie der Universität Heidelberg, 69120 Heidelberg, Germany
[3]Department of Molecular Neurobiology, Max Planck Institute for Medical Research, D-69120 Heidelberg, Germany
[4]Laboratory of Neural Circuits and Plasticity, University of Southern California, Los Angeles, Los Angeles, CA 90089-2520, USA
[5]Apogenix GmbH, 69120 Heidelberg, Germany
[6]Institute of Reconstructive Neurobiology, Life and Brain Center, University of Bonn and Hertie Foundation, D-53127 Bonn, Germany
[7]Medical Research Center, Medical Faculty Mannheim, University of Heidelberg, 68135 Mannheim, Germany
[8]Department of Neuropathology, Institute of Pathology, University of Heidelberg, 69120 Heidelberg, Germany
*Correspondence: a.martin-villalba@dkfz.de
DOI 10.1016/j.stem.2009.05.004

SUMMARY

Adult neurogenesis persists in the subventricular zone and the dentate gyrus and can be induced upon central nervous system injury. However, the final contribution of newborn neurons to neuronal networks is limited. Here we show that in neural stem cells, stimulation of the "death receptor" CD95 does not trigger apoptosis but unexpectedly leads to increased stem cell survival and neuronal specification. These effects are mediated via activation of the Src/PI3K/AKT/mTOR signaling pathway, ultimately leading to a global increase in protein translation. Induction of neurogenesis by CD95 was further confirmed in the ischemic CA1 region, in the naive dentate gyrus, and after forced expression of CD95L in the adult subventricular zone. Lack of hippocampal CD95 resulted in a reduction in neurogenesis and working memory deficits. Following global ischemia, CD95-mediated brain repair rescued behavioral impairment. Thus, we identify the CD95/CD95L system as an instructive signal for ongoing and injury-induced neurogenesis.

INTRODUCTION

In the adult central nervous system (CNS), ongoing neurogenesis persists in two regions, the subventricular zone (SVZ) of the lateral ventricles and the subgranular zone (SGZ) of the hippocampal dentate gyrus (DG) (Lois and Alvarez-Buylla, 1993). In the DG and SVZ, large numbers of neurons are generated from neural stem cells (NSCs), but most die and never integrate into the neuronal circuitry. The number and integration of newly born neurons in the DG can be greatly enhanced by voluntary running, although the exact underlying mechanism remains elusive (Zhao et al., 2008). Also, under pathological conditions such as stroke, proliferation of NSCs increases and newborn neurons migrate to the site of damage (Lindvall et al., 2004). However, in this latter scenario, most of the newly born neurons die, thus rendering the replacement of mature injured neurons inefficient (~0.2%) (Emsley et al., 2005; Arvidsson et al., 2002; Parent et al., 2002). Neurogenesis is enhanced by increased survival and neuronal specification of stem cells or increased survival of newborn neurons. Although survival seems to be such a critical aspect of neurogenesis and NSC function, little is known about the mechanisms and molecules that make stem cells undergo death in the naive or injured brain.

One of the molecules that induces apoptosis after brain injury and in neurodegenerative diseases is CD95 (Fas/APO-1) and its ligand CD95L (Demjen et al., 2004). Recently, CD95 has also emerged as a molecule involved in nonapoptotic signaling (Sancho-Martinez and Martin-Villalba, 2009). In the CNS, CD95L promotes dendritic branching in immature neurons, outgrowth of dorsal root ganglions in vitro, and migration of glioblastoma cells (Desbarats et al., 2003; Kleber et al., 2008; Zuliani et al., 2006).

Here we report that the CD95/CD95L system is an inducer of neurogenesis in the adult brain. CD95 stimulation on NSCs induces differentiation and survival of NSCs. This is mediated by activation of the Src/PI3K/AKT/mTOR signaling pathway, which results in a global increase in protein translation associated with neuronal differentiation. In vivo, CD95-induced neurogenesis is involved in neuronal replacement of ischemic neurons as well as ongoing neurogenesis and working memory formation.

RESULTS

CD95 Induces Neurogenesis by Activating and Supporting Survival of NSCs In Vitro

The CD95 receptor has been well established as an inducer of apoptosis (Krammer, 2000). To study its effect on cultured NSCs, we treated neurosphere cultures with a recombinant

pretrimerized CD95L (CD95L-T4) (see Figure S1 available online). As previously reported (Ricci-Vitiani et al., 2004), CD95 is expressed on human and mouse NSCs (Figures S2A and S2B). When CD95 was stimulated on NSCs, they did not undergo apoptosis (Figures S2C and S2D). Instead, treatment of SVZ NSC cultures with CD95L-T4 increased the number of cells positive for the neuronal marker β-III-tubulin (Figures 1A and 1B). To control for specificity of the observed effect of CD95 on differentiation, we treated NSCs derived from *lpr* mice (Adachi et al., 1993), where CD95 was absent (Figure S2A). In these cells, CD95L-T4 did not induce differentiation, confirming a specific signaling of CD95L-T4 through CD95 (Figure 1C).

We further asked if treatment with CD95L-T4 could enhance differentiation into a neuronal lineage when cells were induced to differentiate by plating and culturing in differentiation medium (Figure 1D). CD95L significantly increased the number of the neuronal markers β-III-tubulin (Figures 1E and 1F), NeuN (Figures 1H and 1I), and calretinin (Figures 1J and 1K) as compared to untreated cells, while the percentage of cells expressing the glial marker GFAP was not changed (Figure 1G). Also in human NSCs, CD95 stimulation resulted in an increased generation of neurons (Figure S2E). The increase in the number of neurons could either be due to an effect of CD95L on differentiation or on proliferation of neuronally committed progenitors. CD95L-T4 treatment did not enhance proliferation, suggesting that the increase in β-III-tubulin-positive cells was rather due to induction of differentiation (Figure S2F).

Neurosphere cultures mainly consist of neural progenitor cells, while putative NSCs are rare (Singec et al., 2006). Therefore, to study the response of actual stem cells to CD95L, we performed a neurosphere assay that specifically addresses the response of putative stem cells to an external factor (Ferron et al., 2007) (Figure 1L). In *wt* NSCs that expressed CD95 (CD95 flox$^{NesCre-}$), but not in CD95-negative NSCs (CD95 flox$^{NesCre+}$), stimulation of CD95 resulted in a significantly higher number of secondary spheres (Figure 1M). The increased number of secondary neurospheres can be the result of increased proliferation or survival of stem cells. The former would imply that secondary spheres from CD95L-T4-treated primary spheres have a higher ratio of NSCs to progenitor cells than their control counterparts and, thus, a resulting higher number of tertiary spheres. The latter implies that the ratio of NSC to progenitor cells within each sphere does not differ between the two groups and, therefore, neither the number of arising tertiary spheres. The fact that CD95 stimulation did not increase secondary neurosphere size (Figure 1O) and no differences in tertiary sphere size (Figure 1P) or number (Figure 1N) were found indicates that CD95L mainly acts on survival and activation/differentiation of NSCs.

CD95 on NSCs Signals through PI3K Activation

How does CD95 increase survival and/or activation of NSCs? Induction of apoptosis via CD95 occurs through the recruitment of the adaptor protein FADD to the death domain (DD) of the CD95. FADD recruitment to CD95 upon treatment with CD95L could not be detected, indicating that FADD seems not to be involved in the pathway inducing differentiation downstream of CD95 (Figure 2A). By contrast, FADD recruitment to CD95 was readily observed in lysates from an ischemic mouse brain (Figure S3A). Also, we did not detect caspase-3 cleavage or caspase activation in NSCs upon CD95 stimulation (Figures S3B and S3C). Lack of FADD recruitment to CD95 upon CD95L stimulation was also observed in glioblastoma cells (Kleber et al., 2008). In these cells, CD95L stimulation induced association of the p85 subunit of PI3K and of the Src family kinase (SFK) member Yes to CD95, finally resulting in activation of the PI3K pathway. Indeed, also in NSCs, PI3K activity, as measured by ELISA-based detection of PI(3,4,5)P3, increased after treatment of cells with CD95L-T4 (Figure 2B). Stimulation of CD95 further resulted in phosphorylation of the PI3K downstream targets AKT and GSK3β (Figure 2C). In NSCs, immunoprecipitation experiments revealed increased association of CD95 with the regulatory p85 subunit of PI3K and the SFK member pp60-src, but not of other SFKs upon CD95 stimulation (Figure 2D and Figure S3B). We further examined the activation state of pp60-src in CD95L-T4-treated and untreated NSCs. Immunoprecipitates of tyrosine phosphorylated proteins were further probed with an antibody that specifically recognizes phosphorylated Y416 in the activation loop of src. pp60-src was phosphorylated and thereby activated 5 min after stimulation with CD95L-T4 (Figure 2E). Further supporting a role for pp60-src in activation of PI3K siRNA, knockdown of pp60-src inhibited CD95L-T4-mediated increase in p85 recruitment to CD95 (Figure 2F). Also, knockdown of pp60-src or a dominant-active form of GSK3β blocked CD95L-T4-mediated increase of β-III-tubulin expression (Figures 2G and 2H). The PI3K inhibitor LY294002 or the SFK inhibitor PP2 blocked CD95-induced GSK3β phosphorylation (Figure 2I). These data indicate that in NSCs, CD95L induces β-III-tubulin expression via the Src/PI3K axis. But what makes NSCs undergo CD95-mediated survival/differentiation and not apoptosis? In glioma cells, we previously reported that knockdown of Yes enables FADD recruitment, and therefore Yes seems to compete with FADD for binding to CD95 (Kleber et al., 2008). Yet knockdown of pp60-src in NSCs did not facilitate recruitment of FADD to CD95 (Figure 2J). This finding suggests the presence of other adaptor molecules and/or post-translational modifications that could prevent FADD binding and therefore apoptosis.

CD95 Stimulation Induces Changes in Gene Expression and a Global Increase in Translation

To further analyze CD95-induced differentiation of NSCs, we performed a translation-state array analysis (TSAA). Total mRNA and polysome-bound mRNA from CD95L-T4-treated and untreated NSCs were extracted and hybridized onto gene microarrays. Despite the fact that 79% of CD95L-regulated polysome-bound transcripts were also differentially regulated in the total fraction (Figure 3A), the higher fold change and mode of regulation of common genes allowed the identification of gene signatures for neurogenesis, protein biosynthesis, and transcription only in the polysomal fraction (Figure 3B). In both fractions, regulated processes involved basal cellular processes participating in cell differentiation as assessed by Gene Ontology Consortium and pathway analysis (Figures 3A and 3B, Figure S4, and Tables S3 and S4). Of the genes that were downregulated in CD95L-treated NSCs, we validated Hes1, Hes5, and Jagged1, three genes involved in Notch signaling using quantitative real-time PCR (Figure 3C). We also validated two genes that were upregulated upon CD95 stimulation in both the total and polysomal

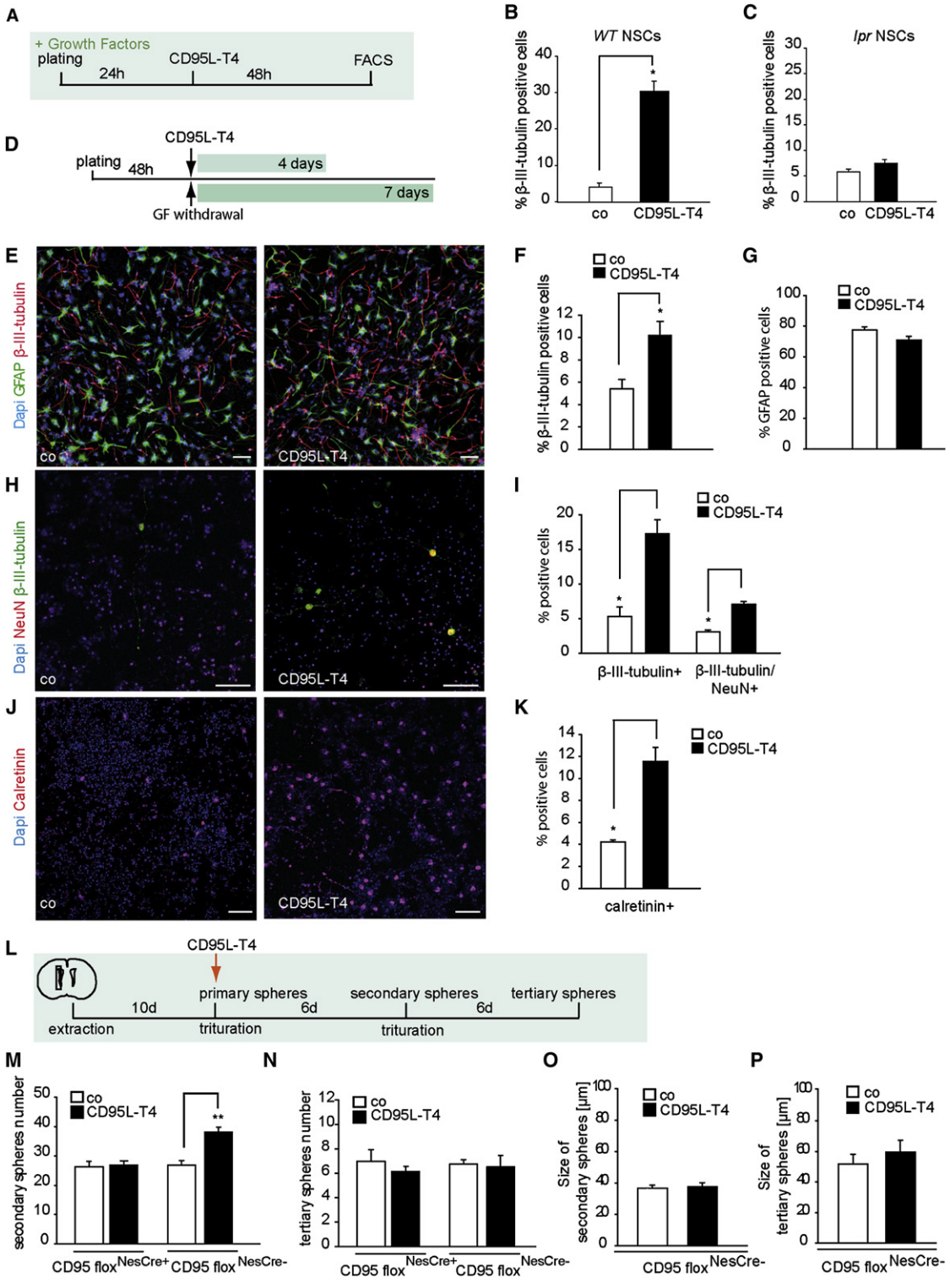

Figure 1. CD95 Stimulation Induces Neuronal Differentiation and Survival of NSCs

(A) Treatment scheme for (B) and (C).

(B and C) (B) FACS quantification of β-III-tubulin-positive NSCs from *wt* (4.22% ± 0.926 versus 30.17% ± 2.8, mean ± SD, n = 4) mice and (C) *lpr* mice.

(D) Treatment scheme for (E)–(K).

(E) Representative pictures of SVZ NSCs cultures differentiated for 4 days in the presence or absence of CD95L-T4.

(F and G) (F) Quantification of β-III-tubulin (4.31% ± 1.25 versus 10.24% ± 2.00, n = 10) and GFAP-expressing cells (G).

fractions known to be crucial for neuronal differentiation: Neurogenin1 (Ngn1), a major proneural transcription factor (Sun et al., 2001), and brain-derived neurotrophic factor (BDNF), which has been shown to mediate survival and differentiation of NSCs (Sairanen et al., 2005) (Figure 3D).

A pathway downstream of PI3K is the mTOR signaling pathway. A hallmark of mTOR signaling is an increase in translation and protein synthesis brought about by phosphorylation and inactivation of its downstream target 4E (eIF4E) binding protein (4EBP), an inhibitor of translation. In murine embryonic stem cells (ESCs) (Sampath et al., 2008), differentiation into embryoid bodies goes along with phosphorylation of 4EBP, thus abolishing the block on translation initiation. Similar to differentiating murine ESCs (Sampath et al., 2008), CD95L-T4 induced a global increase in ribosome-bound mRNA (Figure 4A) and therefore protein translation. CD95 stimulation also resulted in increased phosphorylation of 4EBP (Figure 4B). To address the role of mTOR in CD95-induced neurogenesis, its pharmacological inhibitor Rapamycin was used. Treatment with Rapamycin inhibits 4EBP phosphorylation, thereby increasing the interaction between eIF4E and 4EBP and inhibiting cap-dependent translation (Gingras et al., 2001). The CD95-induced increase in NSCs expressing β-III-tubulin was blocked by Rapamycin (Figure 4C). At the mRNA level, CD95-mediated increase of Ngn1 and decrease of Hes5 mRNA expression was similarly inhibited by Rapamycin (Figures 4D and 4E). By contrast, retinoic acid (RA)-induced decrease of Hes5 mRNA was unaffected by Rapamycin treatment, whereas mRNA levels of Ngn1 were not influenced by RA alone and subsequently neither by treatment with RA and Rapamycin (Figures 4D and 4E). Taken together, TSAA revealed that CD95-induced differentiation does not only result in changes on gene expression known to be important for neuronal differentiation, it also allows the identification of a global differentiation signature and shows that neuronal differentiation is accompanied by increased translation and protein synthesis through the mTOR pathway. Thus, we propose a molecular model for CD95-induced neurogenesis that involves activation of the PI3K/AKT/mTOR and the PI3K/AKT/GSK3β signaling pathways (Figure 4F).

CD95L Overexpression Enhances Neurogenesis in the Adult SVZ

Since CD95L could induce survival and differentiation of NSCs in vitro, we asked if CD95L was also involved in neurogenesis in vivo. We first analyzed expression of CD95 in the adult SVZ. CD95 was detected in Nestin-positive, GFAP-positive, and some DCX-positive cells present in the SVZ, but not DCX-positive cells migrating into the rostral migratory stream (RMS) (Figures 5A–5F and data not shown). Accordingly, fluorescence-activated cell sorting (FACS) of CD95-positive cells from the SVZ revealed that 1.2% of all SVZ cells express CD95. Further, only CD95-expressing cells were able to form neurospheres when plated at a low density (Figures S6G and S6H). The role of CD95L in the SVZ was analyzed by injecting lentiviral vectors carrying CD95L-IRES-GFP or GFP only in the lateral ventricles (Figure 5G). Lentiviral infection was mainly observed in tissue along the ventricle and in the SVZ, and infection rate was comparable in the two groups (data not shown). Mice that were injected with the GFP-only virus showed normal neurogenesis in viral infected areas (Figures 5H–5J). In contrast, in animals injected with CD95L-IRES-GFP, we observed a marked increase in cells expressing Doublecortin (DCX), a marker for immature neurons, in CD95L and GFP-infected areas (Figures 5K–5M). DCX-expressing cells in CD95L-IRES-GFP-infected areas further exhibited a mature morphology with more elaborate processes protruding into the adjacent parenchyma. Importantly, stereological quantification revealed a marked increase in DCX-positive regions upon forced expression of CD95L in the SVZ, a phenomenon often associated with the reported reactive neurogenesis found upon neurodegenerative diseases or ischemic injury to the CNS (Yang and Levison, 2006) (Figures 5N–5P).

CD95 Is Required for Neurogenesis in a Model of Global Ischemia

We further examined the role of CD95 in the reactive neurogenesis induced upon ischemic injury. CD95L is highly upregulated following injury to the CNS (Martin-Villalba et al., 1999). In the mouse model of global ischemia, which is characterized by apoptosis of neurons in the CA1 region of the hippocampus (Martin et al., 2000), CD95L expression was induced as detected by real-time PCR and FACS analysis in the hippocampus 3 days after global ischemia (Figure 6A). Accordingly, when we analyzed tissue from a human patient who suffered from global ischemia resulting from heart failure, we detected CD95L expression in pyramidal neurons in the CA1 region (Figure 6B). In the DG of this patient, CD95 was expressed in few cells in the subgranular layer (Figure 6C). In this region, we also observed Nestin-positive cells that are putative NSCs (Figure 6C). Analysis of the DG in mouse brain slices showed a colocalization of CD95 with GFAP-positive cells (Figure S6D). After global ischemia, the number of existing NSCs seems to be the limiting factor for regeneration, since expansion of NSCs by EGF infusion allows effective regeneration of the injured CA1 region by recruitment of NSCs (Nakatomi et al., 2002). To provide a sufficient number of NSCs, while avoiding confounding effects related to EGF infusion, we transplanted GFP-labeled SVZ NSCs into the brain of

(H–J) Representative pictures of SVZ NSCs cultures differentiated for 7 days in the presence or absence of CD95L-T4. Expression of β-III-tubulin and NeuN (H) and calretinin (J) are depicted. (I) Quantification of β-III-tubulin (5.2883% ± 1.4221 versus 17.3101% ± 1.9818)- and β-III-tubulin/NeuN (3.0661% ± 0.3194 versus 7.1052% ± 0.3979)-expressing cells.

(K) Quantification of calretinin-expressing cells (4.2428% ± 0.1241 versus 11.5439% ± 1.2720).

(L) Treatment scheme for neurosphere assay.

(M) Numbers of secondary spheres from CD95flox$^{NesCre-}$- and CD95flox$^{NesCre+}$-derived NSCs without or with CD95L-T4 treatment (26.83 ± 1.66 versus 38.17 ± 1.54, n = 20).

(N) Numbers of tertiary spheres from CD95flox$^{NesCre-}$- and CD95flox$^{NesCre+}$-derived NSCs without or with CD95L-T4 treatment.

(O) Sizes of secondary and tertiary spheres from CD95flox$^{NesCre-}$-derived NSCs.

(P) Sizes of tertiary spheres from CD95flox$^{NesCre-}$-derived NSCs. Data are depicted as mean ± SEM from at least four biological replicates (Student's t test, *$p < 0.05$; **$p < 0.01$).

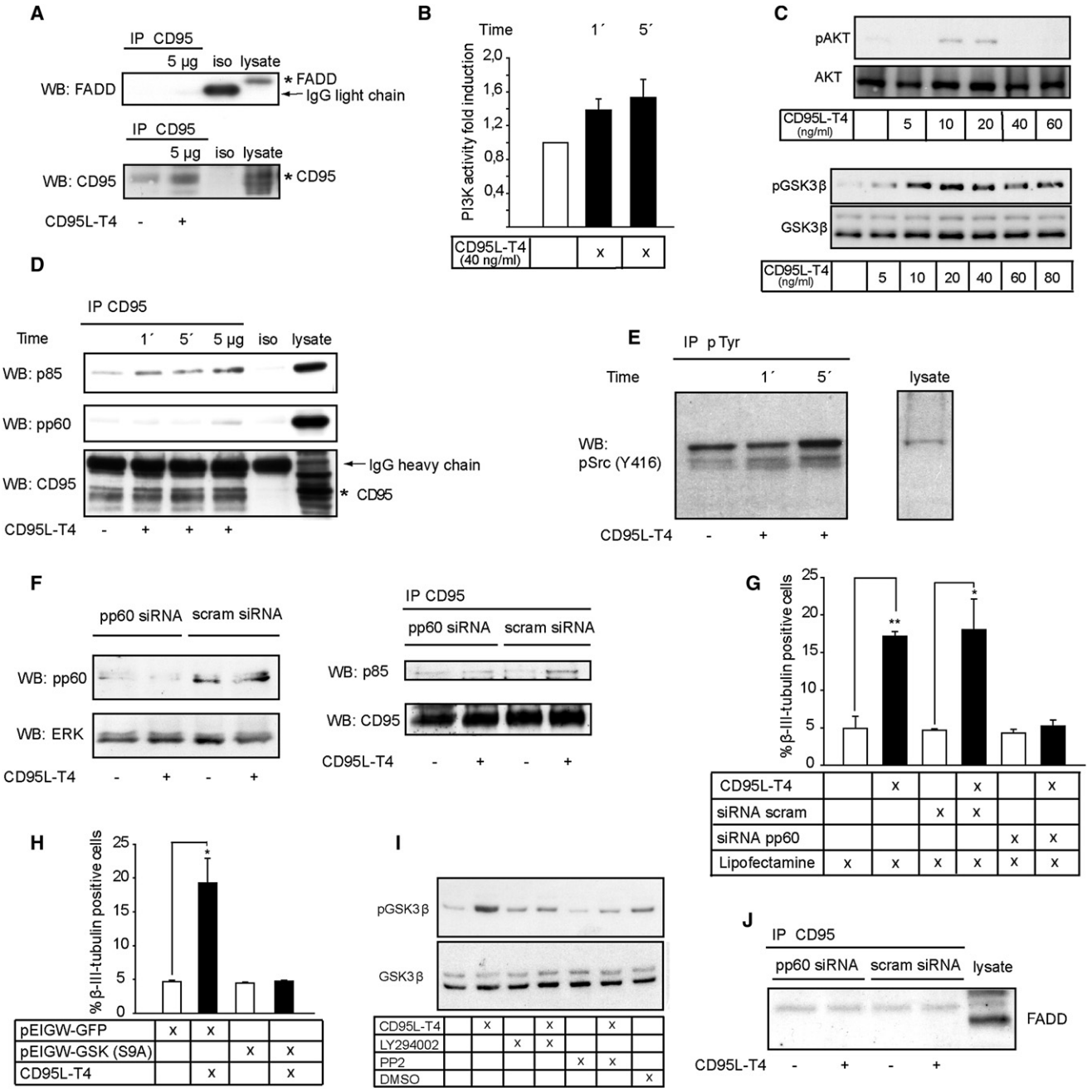

Figure 2. CD95 Stimulation Activates PI3K Signaling through Activation of pp60-src

(A) Lysates from stimulated or nonstimulated SVZ NSCs were analyzed for FADD recruitment. CD95 was immunoprecipitated, and immunoprecipitates were blotted for FADD and CD95. *, specific band.

(B) Changes in PI3K activity were measured by using a photometric PI3K activation kit.

(C) NSCs were stimulated with different concentrations of CD95L-T4, and lysates were blotted for phospho-AKT/PKB (Ser473) or its downstream target phospho-GSK3β (Ser9).

(D) NSCs were stimulated with CD95L-T4. CD95 was immunoprecipitated, and the membranes were probed with anti-p85, anti-pp60-src, and anti-CD95 antibodies. *, specific band.

(E) Anti-phosphotyrosine antibody was used for immunoprecipitation, and immunoprecipitates from CD95L-T4-treated and untreated cells were blotted with an antibody detecting phosphorylated active Src (Y416).

(F) pp60-src knockdown was performed using siRNA and analyzed by western blot (left panel). Immunoprecipitation of CD95 was performed after pp60-src knockdown (right panel).

(G) CD95L-T4-induced differentiation of lipofectamine-treated (4.8900% ± 1.6100 versus 17.1500% ± 0.6500) and scrambled siRNA-treated NSCs (4.6900% ± 0.1600 versus 18.0700% ± 4.0900) was significantly blocked by pp60-Src knockdown (4.3150% ± 0.4350 versus 5.2300% ± 0.7900) as measured by β-III-tubulin expression.

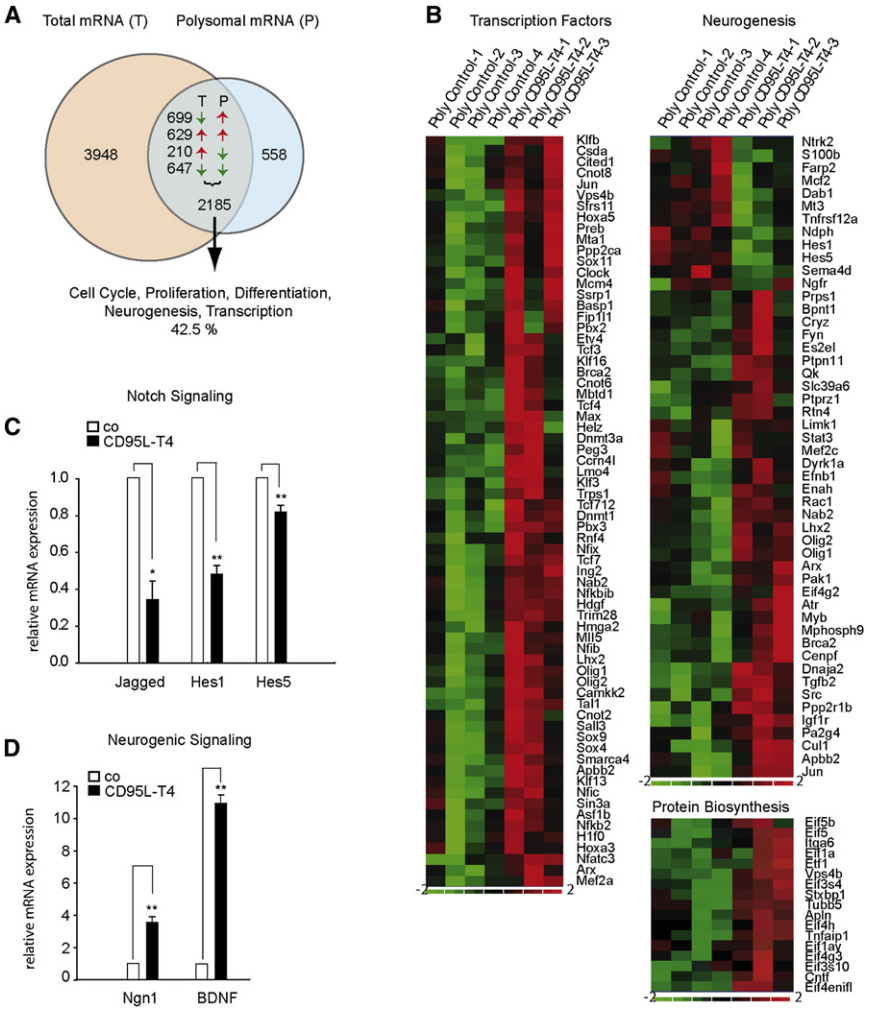

Figure 3. Translation-State Array Analysis of CD95L-Treated and Untreated NSCs

(A) Schematic diagram showing CD95L-dependent gene expression changes at the total and polysomal mRNA levels. Note the differential regulation in the different fractions of common genes (red and green arrows).

(B) Clusters of polysome-bound transcripts involved in transcription, neurogenesis, and protein biosynthesis identified by hierarchical clustering. Color codes are green for downregulated genes, red for upregulated genes, and black for no changes.

(C and D) Validation of microarray data by qRT-PCR of selected CD95L-regulated transcripts. Data are expressed as mean ± SEM of four independent biological samples (Student's t test, *$p < 0.05$; **$p < 0.01$).

injured mice 48 hr after ischemia. Three weeks after injection, we found GFP$^+$ cells in the injured CA1 region. Some of these cells expressed phosphorylated GSK3β, indicating that phosphorylation of GSK3β might play also a role in neuronal differentiation in vivo (Figure 6D). To test if CD95L expressed after ischemia could be involved in neuronal differentiation of transplanted progenitors, we compared SVZ NSCs derived from either *wt* or *lpr* mice (Figure 6E). Notably, 10 weeks after injection, we found GFP$^+$ cells in the CA1 region in mice that received wild-type cells. These cells exhibited a neuronal morphology, and some of these cells expressed the mature neuronal marker NeuN (Figure 6F). In mice that received *lpr* cells, GFP$^+$ cells in the CA1 region were scarce, and only a few cells coexpressed GFP and NeuN (Figures 6F and 6G). The fact that *lpr* NSCs were found in the ischemic region and that in vitro, *lpr* cells could be readily differentiated into neurons when induced to differentiate by plating and cultivating in differentiation medium (data not shown) suggests that they have no intrinsic deficits but that the CD95L/CD95 interaction is required for survival and differentiation of NSCs after global ischemia in the CA1 region.

To test whether transplanted NSCs were functional, we asked if they could improve behavioral deficits associated with hippocampal lesions. The T-maze test is a measure for working memory and crucially dependent on hippocampal function (Deacon and Rawlins, 2006; Whishaw and Tomie, 1996). In this test, a mouse is placed in the start arm and allowed to explore one arm of the maze, while the other arm is blocked (Figure 6H, upper panel). In the next run, the block is removed and the mouse is placed again in the start arm. It can now choose between the previously explored or the novel arm. Rodents prefer the novel arm above chance, a behavior known as spontaneous alternation (Figure 6H, lower panel). Ischemic mice showed significantly reduced success rates in working memory in the T-maze test compared to naive controls (Figure 6I). This defect in spontaneous alternation behavior was rescued in mice injected with *wt* NSCs, indicating that *wt* NSCs are able to integrate into the brain circuitry and improve ischemia-induced deficits. In contrast, mice that received *lpr* NSCs exhibited significantly decreased spontaneous alternation rates comparable to

(H) SVZ NSCs were infected with a lentiviral construct carrying either eGFP alone or a constitutively active mutant of GSK3β (S9→A) and eGFP. Forty-eight hours after stimulation with CD95L-T4, FACS analysis for β-III-tubulin expression of eGFP-positive cells was performed. Cells expressing GFP only showed an increase in β-III-tubulin-positive cells (4.6500 ± 0.2500 versus 19.2750 ± 3.6550), while this was blocked in cells infected with GFP and GSK3β (S9→A) (4.5000 ± 0.1000 versus 4.7100 ± 0.1900).

(I) Treatment with the PI3K inhibitor LY 294002 or the Src inhibitor PP2 reduced CD95L-T4-induced phosphorylation of GSK3β in NSCs.

(J) CD95 was immunoprecipitated from pp60-src siRNA, and scrambled siRNA-treated cells under stimulated and nonstimulated conditions and immunoprecipitates were blotted for FADD. Data in (B), (G), and (H) are expressed as mean ± SEM from each of three independent biological replicates (Student's t test, *$p < 0.05$; **$p < 0.01$).

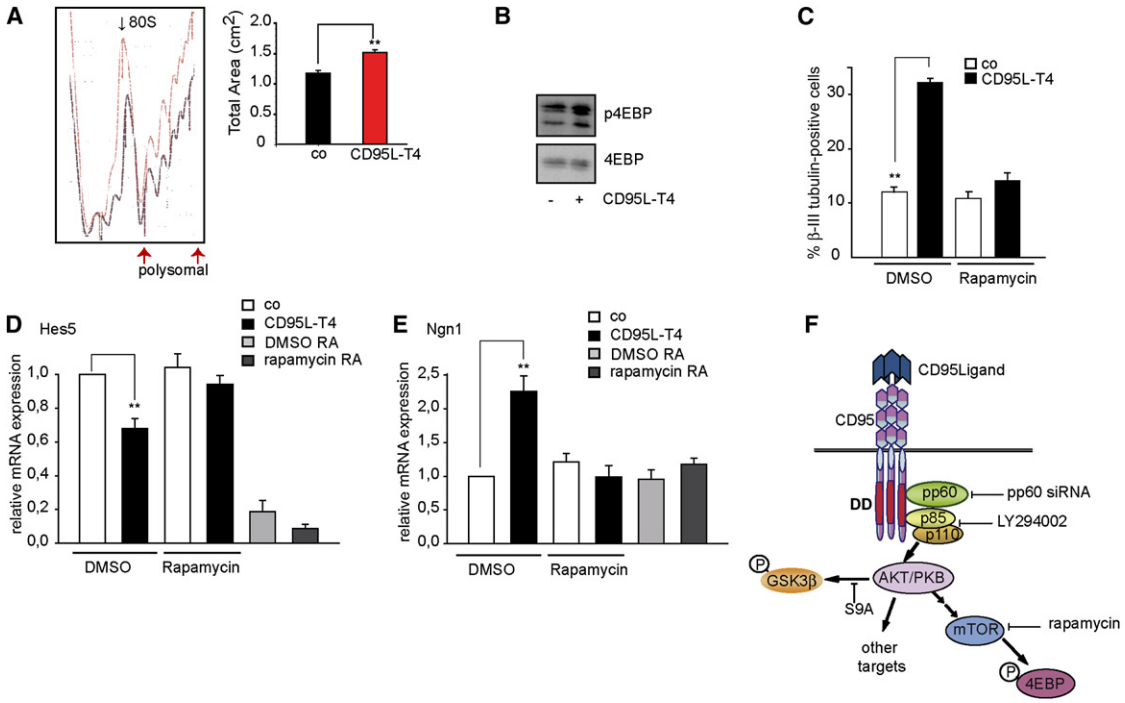

Figure 4. CD95L Induces a Global Increase in Translation

(A) Comparison of polysome profiles of CD95L-T4-treated and untreated SVZ NSCs 48 hr after stimulation and quantification of the area under the curve for monosome and polysome regions.

(B) Western blot depicting phosphorylation of 4EBP upon CD95L-T4 treatment.

(C) Rapamycin treatment abolishes the CD95L-induced increase in β-III-tubulin-positive cells (32.1667% ± 0.7839 versus 14.4667 ± 1.3691).

(D and E) qRT-PCR of selected CD95L-regulated transcripts with or without Rapamycin treatment.

(F) Schematic drawing of proposed signaling events in CD95 signaling in NSCs. Data in (A) and (C) are expressed as mean ± SEM of four independent biological samples; data in (D) and (E) are triplicate samples from three independent biological replicates and are expressed as mean ± SEM (Student's t test, *$p < 0.05$; **$p < 0.01$).

ischemic animals with injection of PBS (Figure 6I). *lpr* NSCs did not integrate into the damaged CA1 and thus were not able to ameliorate behavioral deficits. There were no significant differences between the groups in the motor activity in the open field test, indicating that the effects seen in the spontaneous alternation were not due to changed motor activity or exploratory behavior in the different groups of mice (data not shown).

CD95 Deficiency Results in Reduced Working Memory Formation and Neurogenesis

Recent research suggests that ongoing neurogenesis is an important process for normal hippocampal function. Mice in which neurogenesis has been ablated show deficits in hippocampal-dependent learning tasks such as the Morris water maze and fear conditioning (Drapeau et al., 2003; Dupret et al., 2008; Zhang et al., 2008). Also, *lpr* mice have been shown to exhibit deficits in learning and memory (Sakic et al., 1997) that might be linked to defects in neurogenesis. In *lpr* mice, working memory was analyzed by testing their spontaneous alternation rates in the T-maze (Figure 6H). *lpr* mice exhibited significantly lower success rates in the T-maze compared to *wt* controls (Figure 7B, left). As these mice have a deregulated immune system (Andrews et al., 1978; Sakic et al., 1997), we generated animals lacking CD95 in neural cells while leaving the immune system unaffected (CD95 flox$^{NesCre+}$ mice) to exclude defects related to autoimmune destruction of synapses (Figure S5B). CD95 flox$^{NesCre+}$ mice also showed significantly lower success rates in the T-maze than did control littermates (Figure 7C, left). To further rule out any influence of the previously reported role of CD95 in neuronal development (Zuliani et al., 2006), we studied working memory in CD95 flox^{NesCreERT2} mice in which tamoxifen induced Cre recombination in adult neural stem and progenitor cells. These mice still performed significantly worse in the T-maze compared to their control littermates (Figure 7D). Several studies have shown that wheel running enhances performance of rodents in hippocampal-dependent learning tasks by acting on hippocampal neurogenesis (Van der Borght et al., 2007; van Praag et al., 2005). To corroborate that the observed defect in working memory is due to reduced neurogenesis, we gave *lpr* and CD95 flox$^{NesCre+}$ mice and their respective controls access to a running wheel in their home cage (Figure 7A). Voluntary running rescued the defect exhibited by nonrunner *lpr* and CD95 flox$^{NesCre+}$ mice in T-maze alternation 3 weeks after initiation of running (Figures 7B and 7C). Importantly, 3 months after termination of running, this rescue effect disappeared (Figure 7B, right). The fact that mice with CD95 deletion in adult progenitor cells exhibit deficits in working memory that can be rescued by running, but only momentarily, indicates that working memory is dependent on newly generated neurons and their known higher plasticity as far as they

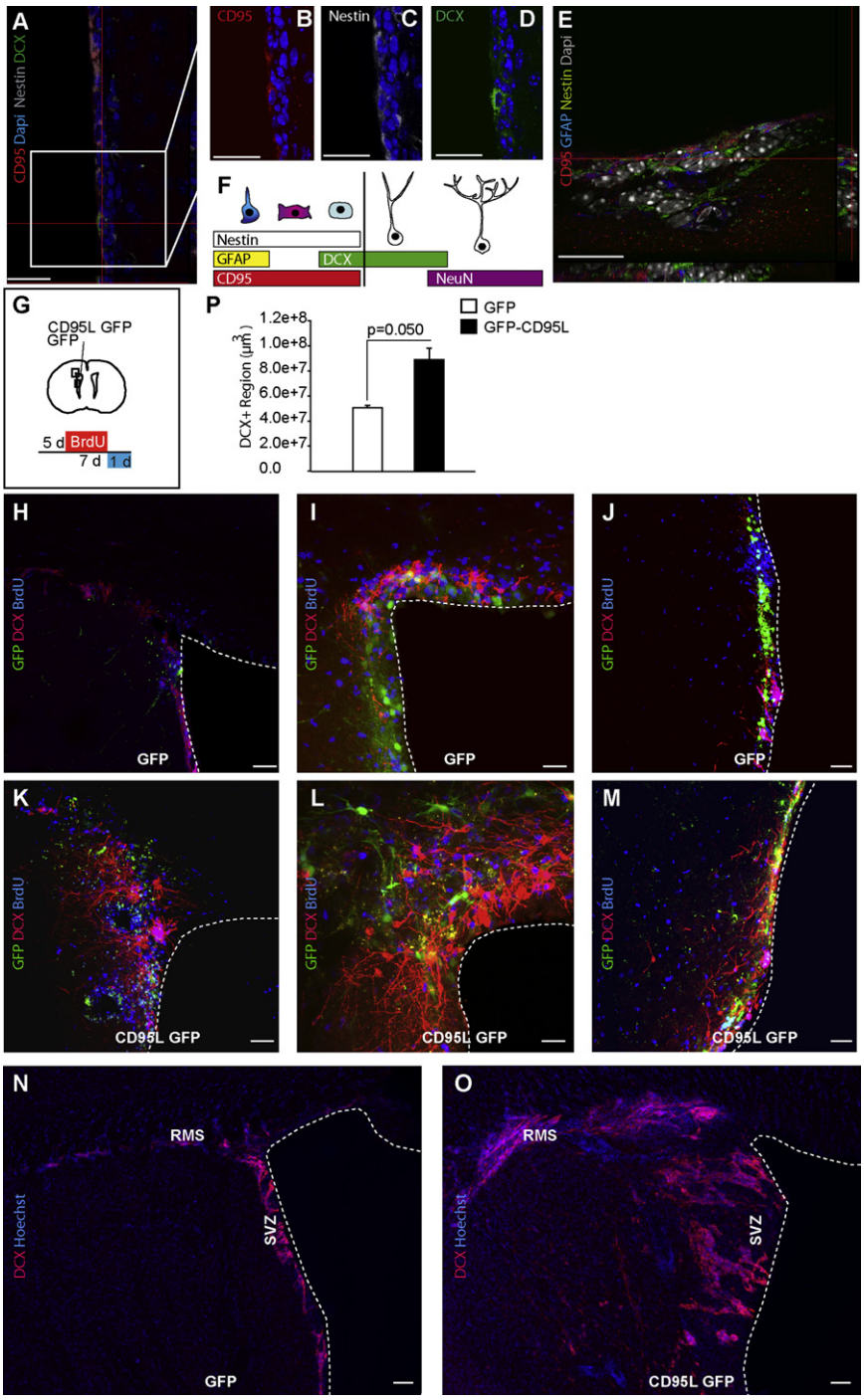

Figure 5. CD95L Expression Induces Neurogenesis In Vivo

(A–E) Confocal images of CD95 expression in the SVZ in cells coexpressing Nestin (C), Doublecortin (DCX) (D), and GFAP (E).

(F) Scheme depicting CD95 expression pattern in NSCs.

(G) Experimental setup for (H)–(O).

(H–J) Representative images of coronal sections of animals injected with a lentivirus expressing GFP.

(K–M) Representative images of coronal sections of animals injected with CD95L- and GFP-expressing LV.

(N) Representative images of sagittal sections of animals injected with a lentivirus expressing GFP.

(O) Representative images of coronal sections of animals injected with a lentivirus expressing CD95L and GFP.

(P) Stereological quantification of DCX-positive regions in animals injected with CD95L-GFP (n = 4) and GFP (n = 2). Scale bar, 50 µm. Data are expressed as mean ± SEM.

are young, and that these neurons can be generated by activation of CD95.

To further confirm that working memory deficits in CD95-deficient mice were indeed due to reduced neurogenesis, the number of newborn neurons was assessed by examining the number of newly generated immature neurons (BrdU/DCX-cells). One day after BrdU administration, *lpr* (Figures 7E and 7G), CD95 flox$^{NesCre+}$ (Figure 7I and Figures S5C and S5D), and CD95 flox$^{NesCreERT2+}$ (Figure 7J) mice showed a significant reduction in BrdU/DCX-positive cells in the DG compared to respective controls. Voluntary running enhanced the number of newly generated immature neurons and subsequently mature ones in both *lpr* and control animals and even compensated for the deficit exhibited by nonrunner *lpr* animals (Figures 7F–7H). Control animals did not show an improvement in working memory performance after running, although they exhibited increased neurogenesis, possibly because a plateau level was reached in the T-maze test. Furthermore, deficiency of CD95 diminishes the number of newborn neurons while leaving the number of BrdU-only cells unaffected (Figure S6A). The decreased number of DCX-positive cells was due to decreased generation and not increased apoptosis, as demonstrated by equivalent numbers of caspase-3-positive cells in *wt* and *lpr* animals (Figure S6C). Importantly, survival of new neurons was not affected by CD95, as shown by the same percentage of surviving mature neurons (BrdU/NeuN cells) in *wt* and *lpr* animals (Figure S6B).

To analyze if behavioral defects could be due to a decrease in branching of immature neurons, we compared the morphology of DCX-positive neurons that also expressed calretinin in CD95flox$^{NesCreERT2-}$ and CD95flox$^{NesCreERT2+}$ mice (Figure S7). Although the overall number of DCX/Calretinin-positive cells was lower in mice lacking CD95 on NSCs, the length and number of dendrites as well as the number of branching points of immature neurons were comparable, indicating that the behavioral deficits in mice lacking CD95 were not due to a decrease in

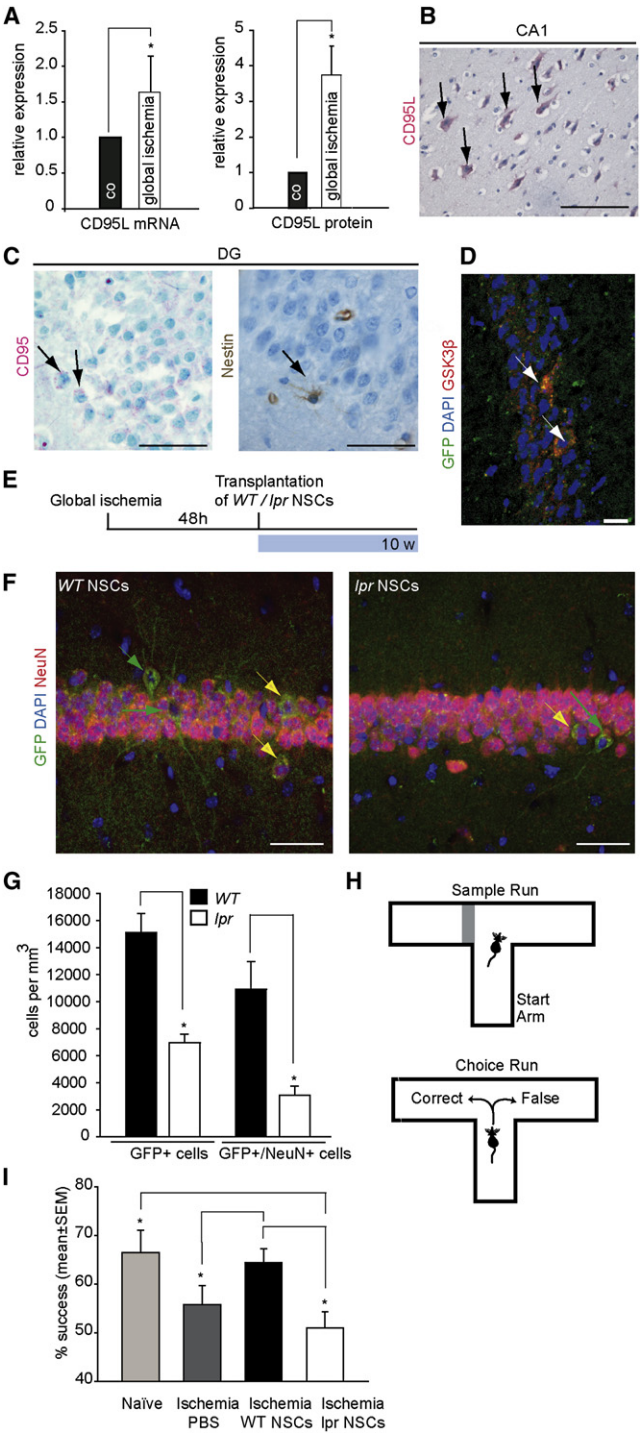

Figure 6. CD95 Is Involved in Injury-Induced Neurogenesis

(A) Three days after global ischemia, CD95L mRNA is upregulated in the hippocampus (1 versus 1.7075 ± 0.1161, n = 4). FACS staining of hippocampal tissue reveals an increase in CD95L-positive cells (1 versus 3.8075 ± 0.4008, n = 4).

(B) Tissue samples from a patient with global ischemia were immunohistochemically analyzed. Cells positive for CD95L (arrows) could be seen in the ischemic CA1 region of the hippocampus.

(C) In the DG of the patient, cells are positive for CD95 (left) and Nestin (right) (arrows).

(D) Three weeks after injection, GFP$^+$ cells are found in the CA1 region of the hippocampus and colocalized with phosphorylated GSK3β (arrows). Scale bar, 15 μm.

(E) Treatment scheme for (F) and (G).

(F) Confocal maximum projections images (z = 15 μm) of the CA1 region of mice transplanted with *wt* or *lpr* NSCs (arrows; green, GFP$^+$/NeuN$^-$; yellow, GFP$^+$/NeuN$^+$).

(G) GFP$^+$ cells in the CA1 region are quantified (lower panel). Brain slices (50 μm) were analyzed in a one-in-six series of sections (250 μm apart). NeuN immunoreactivity was used to measure the volume of the CA1 region. Mice injected with wt NSCs exhibited a higher number of GFP-positive (15133.4682 ± 1396.3 versus 6956.1219 ± 657.1975) and NeuN and GFP double-positive cells (10907.4183 ± 2060.8436 versus 3096.3030 ± 670.9253) in the CA1 region.

(H) Experimental setup of spontaneous alternation.

(I) Global ischemia reduces the success rate in spontaneous alternation (66.44% ± 4.58 versus 55.76% ± 3.9, n = 13). Transplantation of *wt* (64.42% ± 2.77%, n = 13) but not *lpr* NSCs (50.96% ± 3.3, n = 13) rescues the behavioral deficit 5 weeks after injection. Scale bar for all experiments except in (D), 50 μm. Data are expressed as mean ± SEM. Statistics are as follows: Student's t test for (A) and (G); for (I), Kruskal-Wallis analysis (*p < 0.05).

branching of newly born neurons (Figures S7A and S7B). In the naive adult hippocampus, CD95 and CD95L were expressed in cells of the subgranular layer of the DG that exhibited a radial glia-like morphology and expressed GFAP—putative NSCs (Figures S6D–S6F). Accordingly, CD95 sorting of hippocampal cells revealed that only CD95-positive but not CD95-negative cells form neurospheres when seeded at a low density, suggesting that they are putative NSCs (Figure S6H).

DISCUSSION

Apoptosis, Neurogenesis, and the Death Receptor CD95

Here we report that a "death receptor" increases survival and neuronal differentiation of NSCs. That a factor in charge of driving damaged cells into apoptosis is also involved in their replacement by newborn cells is not surprising, given that apoptosis and neurogenesis go hand in hand. Already Magavi and colleagues showed that neurogenesis can be readily induced in the non-neurogenic cortex if selective apoptosis of cortical neurons is triggered (Magavi et al., 2000). Apoptosis and neurogenesis are also closely related in ongoing hippocampal neurogenesis. Many progenitor cells are born in the hippocampus every day, but only a small fraction survives and integrates in the neuronal circuitry (Aimone et al., 2006; Zhao et al., 2008). Furthermore, learning promotes apoptosis of superfluous DCX-positive cells, and blocking of apoptosis impairs learning (Dupret et al., 2007). Likewise, upon brain injury or neurodegenerative disease, neural progenitors in the SVZ proliferate, resulting in an expansion of the SVZ. In our study, we observed a similar broadening of the SVZ when we injected CD95L-expressing lentivirus in the lateral ventricles. Finally, following global ischemia, selective apoptosis of ischemic CA1 neurons allows efficient neuronal replacement by newly born neurons. In summary, CD95-induced neurogenesis goes along with apoptosis.

CD95-Induced NSC Differentiation Is Characterized by Activation of PI3K and an Increase in Protein Synthesis and Translation

Our data show that in NSCs CD95 does not induce apoptosis but results in activation of the Src/PI3K/GSK3β-mTOR pathway.

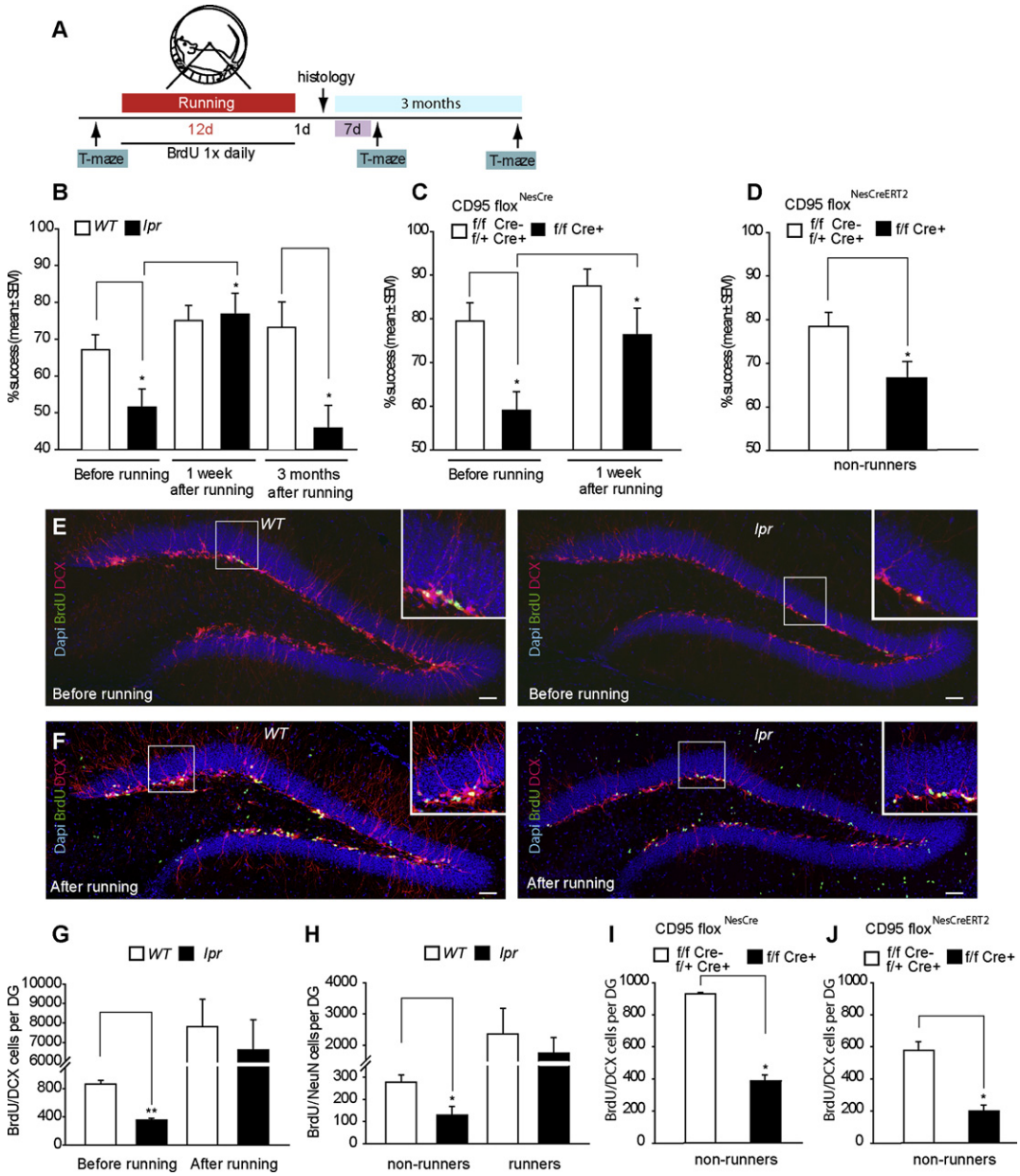

Figure 7. CD95 on Neural Progenitor Cells Is Involved in Working Memory and Neurogenesis

(A) Timeline of the experiments performed.

(B) *lpr* mice show significantly reduced success rates in the T-maze performance compared to *wt* controls (51.78% ± 4.13 versus 67.19% ± 3.864). Running rescues deficits in the working memory performance of *lpr* mice (76.79% ± 4.13). Three months after the end of the running period, *lpr* mice show again significantly reduced success rates in the T-maze (73.2143% ± 6.9160% versus 45.8333% ± 6.1802).

(C) CD95 flox$^{NesCre+}$ (f/f Cre+) mice had a reduced success rate in spontaneous alternation (59.03% ± 4.31 versus 79.46% ± 4.25) compared to control littermates (f/f Cre− and f/+ Cre+). Success rates of Cre+ mice reached the level of control mice 1 week after wheel running (76.39% ± 6.05).

(D) CD95 flox$^{NesCreERT2+}$ mice (Cre+) performed worse in the T-maze than did their control littermates (f/f Cre− and f/+ Cre+) (66.67% ± 3.33 versus 78.33% ± 3.63).

(E and F) Representative images of DG neurogenesis of *lpr* and *wt* mice; nonrunners (E) and runners (F).

(G–I) Stereological quantification of neurogenesis (G) *lpr* mice showed significantly reduced numbers of newborn immature neurons (BrdU/DCX) at 24 hr after injection of BrdU (356.1 ± 26.69 versus 862.02 ± 55.33, n = 5) . After running, *lpr* and *wt* mice had similar numbers of BrdU/DCX cells. (H) The 4 week survival of generated neurons (BrdU/NeuN-cells) was significantly reduced in *lpr* mice compared to *wt* mice (129.69 ± 39.34 versus 278.16 ± 32.49, n = 6) and enhanced by voluntary running. (I) CD95flox$^{NesCre+}$ mice show reduced numbers of DCX/BrdU-cells 24 hr after injection of BrdU compared to control littermates (389.34 ± 34.57 versus 929.89 ± 8.58, n = 5).

(J) CD95flox$^{NesCreERT2+}$ mice show reduced numbers of DCX/BrdU-cells 24 hr after injection of BrdU compared to control littermates (577.9256 ± 59.2357 versus 197.8116 ± 41.1549, n = 5). f, flox; DG, dentate gyrus. Scale bars, 50 μm. Data are expressed as mean ± SEM. Statistics are as follows: multiway ANOVA followed by Holm-Sidak for (B) and (C); Student's t test for (G)–(J) (*$p < 0.05$; **$p < 0.001$).

In the past, several reports have pointed out an important role for PI3K in CD95-induced signaling (Eischen et al., 1994; Schlottmann et al., 1996). These reports, however, suggested that CD95-induced tyrosine phosphorylation is a prerequisite for CD95-mediated apoptosis. Likewise, the phosphatases SHP-1, SHP-2, and SHIP were found to associate with CD95 to counteract survival-factor-initiated pathways (Daigle et al., 2002). In glioblastoma cells, however, we found that the SFK kinase Yes, and not pp60-src, as in NSCs, is recruited to CD95 together with the PI3K subunit p85, resulting in activation of AKT to signal invasion and not apoptosis (Kleber et al., 2008). Thus, in glioblastoma cells and NSCs, different mediators lead to PI3K activation to increase tumorigenesis or neurogenesis, respectively. This finding might support one aspect of the cancer stem cell theory: that at least some cells found in glioblastoma share some signaling pathways with NSCs.

A downstream effector of PI3K is mTor and its target 4EBP. 4EBP competes with eIF4G for binding to eIF4E, thus preventing translation. Phosphorylation of 4EBP is thought to inactivate it and enhance initiation of translation and ribosome biogenesis. In ESCs, it has recently been shown (Sampath et al., 2008) that differentiation is characterized by a global increase in mRNA transcript abundance, polysome content, protein synthesis, and protein content controlled by several translational regulators including mTOR and its target 4EBP. This "anabolic switch" is also found in CD95L-induced differentiation of NSCs. Further, analysis of polysome-bound transcripts revealed changes on transcripts involved in cell differentiation, development, and neurogenesis. Taken together, TSAA shows that CD95L evokes changes on translation similar to ESC differentiation, and it also suggests that regulation of ESC and NSC differentiation have much in common.

CD95 and Running and Working Memory

We found that loss of CD95 expression on NSCs resulted in decreased working memory performance and that mice lacking CD95 exhibited reduced neurogenesis. The link between normal hippocampal function and neurogenesis has been recently established by studies in mice in which neurogenesis has been ablated: these animals exhibit difficulties in hippocampal-dependent learning tasks such as the Morris water maze and fear conditioning (Drapeau et al., 2003; Dupret et al., 2007; Zhang et al., 2008). In this manuscript, we focus on elucidating the role of CD95-induced hippocampal neurogenesis in hippocampal-dependent spatial/contextual working memory. This is only reliably shown by testing animals on the T-Maze paradigm. Previous studies have shown that acquisition of spatial memory (water maze) and contextual fear conditioning do not require stem cell activity (Shors, 2008). With regard to spatial memory, it has been shown that animals can learn to navigate space and emit the appropriate operant response with very few if any newly generated neurons (Shors, 2008). Likewise, animals can readily learn to fear a context despite a scarce number of new neurons (Shors et al., 2002). Also, genetic deletion of TLX in adult NSCs resulted in a significant reduction of stem cells and suppression of neurogenesis that did not affect contextual fear conditioning (Zhang et al., 2008). In addition, repetitive training in spatial learning tasks could prevent death of newly generated neurons and therefore confound the studies that aim to distinguish the role of neurogenesis versus neural survival for behavioral function (Gould et al., 1999; Sisti et al., 2007). Notably, in our work the rescue of spontaneous T-maze alternation by voluntary running provides evidence that ongoing neurogenesis specifically tunes working memory. It is believed that less-specific firing of newborn neurons, possibly due to presence of action-potential boosting calcium spikes or GABA-mediated membrane depolarization, may help to encode information about unrelated events, which occur close in time, into overlapping subsets of CA3 (Aimone et al., 2006; Lledo et al., 2006). Our data show that the number of these young neurons can be modulated after voluntary physical experience. Interestingly, although the number of neurons was increased only 1 day after completion of voluntary running, this was not sufficient to rescue the working memory deficit at that time. Moreover, running-elicited rescue of working memory deficits disappeared at later time points. This suggests that integration of these neurons into functional circuits during a critical period mediates their role in working memory formation.

We have previously demonstrated that stimulation of CD95 on hippocampal and cortical developing neurons increases the formation of branches (Zuliani et al., 2006). However, in the hippocampal DG, CD95 is expressed in GFAP-positive cells with radial glial morphology, but not in newly born neurons. Besides, the number of branches of DCX/calretinin-positive neurons was comparable in *wt* and mutant mice. These data indicate that the effect of CD95 in hippocampal-dependent working memory is not related to CD95-induced branching. A possible alternative explanation of the working memory deficits exhibited by mice with deletion of CD95 in NSC might be that the CD95L-exposed NSC supports the "well-being" of the newborn neurons by providing a better extracellular niche. This could occur via the secretion of survival-promoting factors, e.g., by secretion of BNDF, which we found highly upregulated in NSCs upon CD95L stimulation.

CD95 for Brain Repair

We have demonstrated that following global ischemia the CD95/CD95L interaction supports neurogenesis. CD95L can kill damaged neurons (Martin-Villalba et al., 1999), promote their replacement by neural progenitor cells, and even support further maturation of these newly generated neurons (Zuliani et al., 2006). Following global ischemia, however, the number of newly generated endogenous NSCs seems to be the limiting factor, as EGF and bFGF-induced expansion of NSCs allowed for partial recovery of ischemia-induced spatial learning deficits (Nakatomi et al., 2002). If CD95L induces neurogenesis and is upregulated in the diseased brain, why is neurogenesis after injury in most cases not more pronounced? At the time at which CD95L has its highest expression—the acute injury phase—apoptosis is in most cases associated with massive induction of necrosis, inflammation, and production of reactive oxygen species (ROS). Unravelling the factors blocking CD95-mediated neurogenesis in the context of ischemia and neurodegeneration will enable the use of CD95 to harness endogenously generated NSCs to repair the diseased CNS.

EXPERIMENTAL PROCEDURES

Animals

Animals used are described in Table S1. C57BL/6J mice were bought from Charles River Laboratories. *lpr* mice (Adachi et al., 1993) were backcrossed more than ten generations to C57BL/6J. CD95 floxed mice were bred with Nestin-Cre or Nestin-CreERT2 mice. Eight-week old Nestin-CreERT2 mice and respective controls (heterozygous and Cre−) were i.p. injected twice a day for 5 days with tamoxifen (2 mg/day). All animal experiments were performed in accordance with the institutional guidelines of the German Cancer Research Center and were approved by the Regierungspräsidium Karlsruhe, Germany.

Behavioral Tests

Behavioral tests were performed as described before (Deacon and Rawlins, 2006). For details, see the Supplemental Data.

In Vivo Neurogenesis

Age-matched CD95 flox$^{NesCre+}$ and CD95 flox$^{NesCre-}$ mice or *wt* and *lpr* mice were injected with 300 mg/kg BrdU and perfused 24 hr after to analyze BrdU/DCX-positive cells (n = 5), or alternatively, mice were injected on three consecutive days with 300 mg/kg BrdU and perfused 4 weeks after to analyze BrdU/NeuN-positive cells (n = 6). To analyze activity-dependent neurogenesis in *lpr* and *wt* mice, mice were injected for 12 consecutive days with BrdU (50 mg/kg). During this time, animals had access to a running wheel. Animals were perfused 1 day after to analyze BrdU/DCX, or alternatively, mice had another 4 weeks' access to a running wheel and were perfused afterwards to analyze BrdU/NeuN-positive cells (n = 5). For each animal, confocal stacks (30 μm each) of six vibratome coronal brain slices (50 μm thick, 250 μm apart) were acquired, and cells were counted. Cell numbers were normalized to the area of the DG.

Global Ischemia and Neural Stem Cell Transplantation

Briefly, 12-week-old female C57BL6 mice were anesthetized, and common carotoid arteries were exposed. Both carotoid arteries were occluded using microclamps (Fine Science Tools). After 10 min, clamps were removed, and the wound was closed. Forty-eight hours after global ischemia induction, mice were anesthetized. Lentiviral infected NSCs were trypsinized, washed in PBS, and resuspended at a concentration of 250,000 cells per μl medium. Of the cell suspension, 2 μl was injected into the striatum using a Flexi-fill syringe and a Micro4 syringe pump controller (World Precision Instruments) at a rate of 200 nl/min. For histology, FACS analysis, or real-time PCR, 3 mice per group were used; for behavioral tests, 13 mice per group were used.

Translation-State and Microarray Analysis

Polysomal-bound and total RNA were isolated as described (Diehn et al., 2000) and hybridized to Affymetrix GeneChip MOE430A2. For detailed experimental procedures, see the Supplemental Data. Array data are publicly available at GEO GSE15623.

Statistical Analysis

All results, unless otherwise stated, were analyzed by using Student's t test. Data in Figures 6I, 7B, and 7C were tested for statistical significance using multiway ANOVA, and post hoc pairwise comparisons were performed using Holm-Sidak test after correcting the p value (<0.05) for repeated comparisons using Bonferroni correction method. All data are presented as mean ± standard error (SEM), unless otherwise stated.

SUPPLEMENTAL DATA

Supplemental Data include Supplemental Experimental Procedures, seven figures, four tables, and Supplemental References and can be found with the article online at http://www.cell.com/cell-stem-cell/supplemental/S1934-5909(09)00213-6.

ACKNOWLEDGMENTS

We thank Günther Schütz for the Nestin-Cre and Nestin-CreERT2 mouse lines. We thank Klaus Rajewski for the CD95flox mouse line. Support by the DKFZ Light Microscopy Facility and the Nikon Imaging Center at the University of Heidelberg is gratefully acknowledged. We thank Trevor C. Dale and Till Wenger for plasmid constructs. We further thank Alexandra Beisel and Jennifer Hermes for excellent technical support. This work was supported by the German Research Foundation (DFG), the German Federal Ministry of Education and Research (BMBF), and Systems Biology of Signaling in Cancer (Helmholtz Alliance on Systems Biology).

Received: October 9, 2008
Revised: February 9, 2009
Accepted: May 7, 2009
Published: August 6, 2009

REFERENCES

Adachi, M., Watanabe-Fukunaga, R., and Nagata, S. (1993). Aberrant transcription caused by the insertion of an early transposable element in an intron of the Fas antigen gene of lpr mice. Proc. Natl. Acad. Sci. USA *90*, 1756–1760.

Aimone, J.B., Wiles, J., and Gage, F.H. (2006). Potential role for adult neurogenesis in the encoding of time in new memories. Nat. Neurosci. *9*, 723–727.

Andrews, B.S., Eisenberg, R.A., Theofilopoulos, A.N., Izui, S., Wilson, C.B., McConahey, P.J., Murphy, E.D., Roths, J.B., and Dixon, F.J. (1978). Spontaneous murine lupus-like syndromes. Clinical and immunopathological manifestations in several strains. J. Exp. Med. *148*, 1198–1215.

Arvidsson, A., Collin, T., Kirik, D., Kokaia, Z., and Lindvall, O. (2002). Neuronal replacement from endogenous precursors in the adult brain after stroke. Nat. Med. *8*, 963–970.

Daigle, I., Yousefi, S., Colonna, M., Green, D.R., and Simon, H.U. (2002). Death receptors bind SHP-1 and block cytokine-induced anti-apoptotic signaling in neutrophils. Nat. Med. *8*, 61–67.

Deacon, R.M., and Rawlins, J.N. (2006). T-maze alternation in the rodent. Nat. Protocols *1*, 7–12.

Demjen, D., Klussmann, S., Kleber, S., Zuliani, C., Stieltjes, B., Metzger, C., Hirt, U.A., Walczak, H., Falk, W., Essig, M., et al. (2004). Neutralization of CD95 ligand promotes regeneration and functional recovery after spinal cord injury. Nat. Med. *10*, 389–395.

Desbarats, J., Birge, R.B., Mimouni-Rongy, M., Weinstein, D.E., Palerme, J.S., and Newell, M.K. (2003). Fas engagement induces neurite growth through ERK activation and p35 upregulation. Nat. Cell Biol. *5*, 118–125.

Diehn, M., Eisen, M.B., Botstein, D., and Brown, P.O. (2000). Large-scale identification of secreted and membrane-associated gene products using DNA microarrays. Nat. Genet. *25*, 58–62.

Drapeau, E., Mayo, W., Aurousseau, C., Le, M.M., Piazza, P.V., and Abrous, D.N. (2003). Spatial memory performances of aged rats in the water maze predict levels of hippocampal neurogenesis. Proc. Natl. Acad. Sci. USA *100*, 14385–14390.

Dupret, D., Fabre, A., Dobrossy, M.D., Panatier, A., Rodriguez, J.J., Lamarque, S., Lemaire, V., Oliet, S.H., Piazza, P.V., and Abrous, D.N. (2007). Spatial learning depends on both the addition and removal of new hippocampal neurons. PLoS Biol. *5*, e214. 10.1371/journal.pbio.0050214.

Dupret, D., Revest, J.M., Koehl, M., Ichas, F., De, G.F., Costet, P., Abrous, D.N., and Piazza, P.V. (2008). Spatial relational memory requires hippocampal adult neurogenesis. PLoS ONE *3*, e1959. 10.1371/journal.pone.0001959.

Eischen, C.M., Dick, C.J., and Leibson, P.J. (1994). Tyrosine kinase activation provides an early and requisite signal for Fas-induced apoptosis. J. Immunol. *153*, 1947–1954.

Emsley, J.G., Mitchell, B.D., Kempermann, G., and Macklis, J.D. (2005). Adult neurogenesis and repair of the adult CNS with neural progenitors, precursors, and stem cells. Prog. Neurobiol. *75*, 321–341.

Ferron, S.R., Andreu-Agullo, C., Mira, H., Sanchez, P., Marques-Torrejon, M.A., and Farinas, I. (2007). A combined ex/in vivo assay to detect effects of exogenously added factors in neural stem cells. Nat. Protoc. *2*, 849–859.

Gingras, A.C., Raught, B., and Sonenberg, N. (2001). Regulation of translation initiation by FRAP/mTOR. Genes Dev. *15*, 807–826.

Gould, E., Beylin, A., Tanapat, P., Reeves, A., and Shors, T.J. (1999). Learning enhances adult neurogenesis in the hippocampal formation. Nat. Neurosci. *2*, 260–265.

Kleber, S., Sancho-Martinez, I., Wiestler, B., Beisel, A., Gieffers, C., Hill, O., Thiemann, M., Mueller, W., Sykora, J., Kuhn, A., et al. (2008). Yes and PI3K bind CD95 to signal invasion of glioblastoma. Cancer Cell *13*, 235–248.

Krammer, P.H. (2000). CD95's deadly mission in the immune system. Nature *407*, 789–795.

Lindvall, O., Kokaia, Z., and Martinez-Serrano, A. (2004). Stem cell therapy for human neurodegenerative disorders-how to make it work. Nat. Med. *10* (*Suppl*), S42–S50.

Lledo, P.M., Alonso, M., and Grubb, M.S. (2006). Adult neurogenesis and functional plasticity in neuronal circuits. Nat. Rev. Neurosci. *7*, 179–193.

Lois, C., and Alvarez-Buylla, A. (1993). Proliferating subventricular zone cells in the adult mammalian forebrain can differentiate into neurons and glia. Proc. Natl. Acad. Sci. USA *90*, 2074–2077.

Magavi, S.S., Leavitt, B.R., and Macklis, J.D. (2000). Induction of neurogenesis in the neocortex of adult mice. Nature *405*, 951–955.

Martin, L.J., Sieber, F.E., and Traystman, R.J. (2000). Apoptosis and necrosis occur in separate neuronal populations in hippocampus and cerebellum after ischemia and are associated with differential alterations in metabotropic glutamate receptor signaling pathways 10. J. Cereb. Blood Flow Metab. *20*, 153–167.

Martin-Villalba, A., Herr, I., Jeremias, I., Hahne, M., Brandt, R., Vogel, J., Schenkel, J., Herdegen, T., and Debatin, K.M. (1999). CD95 ligand (Fas-L/APO-1L) and tumor necrosis factor-related apoptosis-inducing ligand mediate ischemia-induced apoptosis in neurons. J. Neurosci. *19*, 3809–3817.

Nakatomi, H., Kuriu, T., Okabe, S., Yamamoto, S., Hatano, O., Kawahara, N., Tamura, A., Kirino, T., and Nakafuku, M. (2002). Regeneration of hippocampal pyramidal neurons after ischemic brain injury by recruitment of endogenous neural progenitors. Cell *110*, 429–441.

Parent, J.M., Vexler, Z.S., Gong, C., Derugin, N., and Ferriero, D.M. (2002). Rat forebrain neurogenesis and striatal neuron replacement after focal stroke. Ann. Neurol. *52*, 802–813.

Ricci-Vitiani, L., Pedini, F., Mollinari, C., Condorelli, G., Bonci, D., Bez, A., Colombo, A., Parati, E., Peschle, C., and De Maria, R. (2004). Absence of caspase 8 and high expression of PED protect primitive neural cells from cell death. J. Exp. Med. *200*, 1257–1266.

Sairanen, M., Lucas, G., Ernfors, P., Castren, M., and Castren, E. (2005). Brain-derived neurotrophic factor and antidepressant drugs have different but coordinated effects on neuronal turnover, proliferation, and survival in the adult dentate gyrus. J. Neurosci. *25*, 1089–1094.

Sakic, B., Szechtman, H., and Denburg, J.A. (1997). Neurobehavioral alterations in autoimmune mice. Neurosci. Biobehav. Rev. *21*, 327–340.

Sampath, P., Pritchard, D.K., Pabon, L., Reinecke, H., Schwartz, S.M., Morris, D.R., and Murry, C.E. (2008). A hierarchical network controls protein translation during murine embryonic stem cell self-renewal and differentiation. Cell Stem Cell *2*, 448–460.

Sancho-Martinez, I., and Martin-Villalba, A. (2009). Tyrosine phosphorylation and CD95: a FAScinating switch. Cell Cycle *8*, 838–842.

Schlottmann, K.E., Gulbins, E., Lau, S.M., and Coggeshall, K.M. (1996). Activation of Src-family tyrosine kinases during Fas-induced apoptosis. J. Leukoc. Biol. *60*, 546–554.

Shors, T.J. (2008). From stem cells to grandmother cells: how neurogenesis relates to learning and memory. Cell Stem Cell *3*, 253–258.

Shors, T.J., Townsend, D.A., Zhao, M., Kozorovitskiy, Y., and Gould, E. (2002). Neurogenesis may relate to some but not all types of hippocampal-dependent learning. Hippocampus *12*, 578–584.

Singec, I., Knoth, R., Meyer, R.P., Maciaczyk, J., Volk, B., Nikkhah, G., Frotscher, M., and Snyder, E.Y. (2006). Defining the actual sensitivity and specificity of the neurosphere assay in stem cell biology. Nat. Methods *3*, 801–806.

Sisti, H.M., Glass, A.L., and Shors, T.J. (2007). Neurogenesis and the spacing effect: learning over time enhances memory and the survival of new neurons. Learn. Mem. *14*, 368–375.

Sun, Y., Nadal-Vicens, M., Misono, S., Lin, M.Z., Zubiaga, A., Hua, X., Fan, G., and Greenberg, M.E. (2001). Neurogenin promotes neurogenesis and inhibits glial differentiation by independent mechanisms. Cell *104*, 365–376.

Van der Borght, K., Havekes, R., Bos, T., Eggen, B.J., and Van der Zee, E.A. (2007). Exercise improves memory acquisition and retrieval in the Y-maze task: relationship with hippocampal neurogenesis. Behav. Neurosci. *121*, 324–334.

van Praag, H., Shubert, T., Zhao, C., and Gage, F.H. (2005). Exercise enhances learning and hippocampal neurogenesis in aged mice. J. Neurosci. *25*, 8680–8685.

Whishaw, I.Q., and Tomie, J.A. (1996). Of mice and mazes: similarities between mice and rats on dry land but not water mazes. Physiol. Behav. *60*, 1191–1197.

Yang, Z., and Levison, S.W. (2006). Hypoxia/ischemia expands the regenerative capacity of progenitors in the perinatal subventricular zone. Neuroscience *139*, 555–564.

Zhang, C.L., Zou, Y., He, W., Gage, F.H., and Evans, R.M. (2008). A role for adult TLX-positive neural stem cells in learning and behaviour. Nature *451*, 1004–1007.

Zhao, C., Deng, W., and Gage, F.H. (2008). Mechanisms and functional implications of adult neurogenesis. Cell *132*, 645–660.

Zuliani, C., Kleber, S., Klussmann, S., Wenger, T., Kenzelmann, M., Schreglmann, N., Martinez, A., Del Rio, J.A., Soriano, E., Vodrazka, P., et al. (2006). Control of neuronal branching by the death receptor CD95 (Fas/Apo-1). Cell Death Differ. *13*, 31–40.